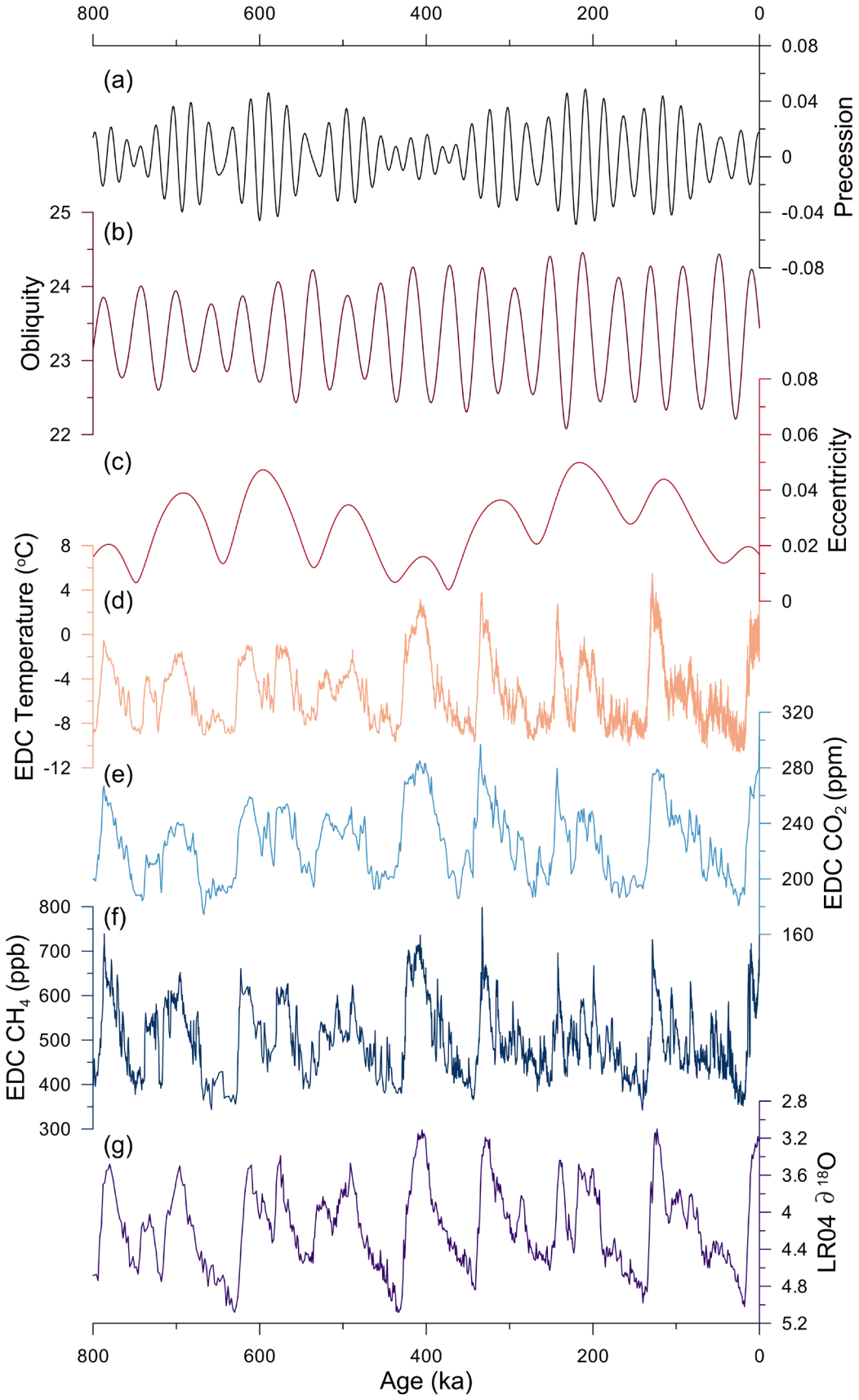

Figure 1 – Orbital forcing and climate records for the last 800 kyr. a, Precession. **b,** Obliquity. **c,** Eccentricity (. **d,** Deuterium-derived temperature from the EPICA Dome C ice core in Antarctica (Jouzel et al., 2007). **e,** Atmospheric CO_2 from EPICA Dome C (EPICA community members, 2007, Lüthi et al., 2008). **f,** Atmospheric CH_4 from EPICA Dome C (EPICA community members, 2007). **g,** Global benthic oxygen isotope stack (Lisiecki and Raymo, 2005).

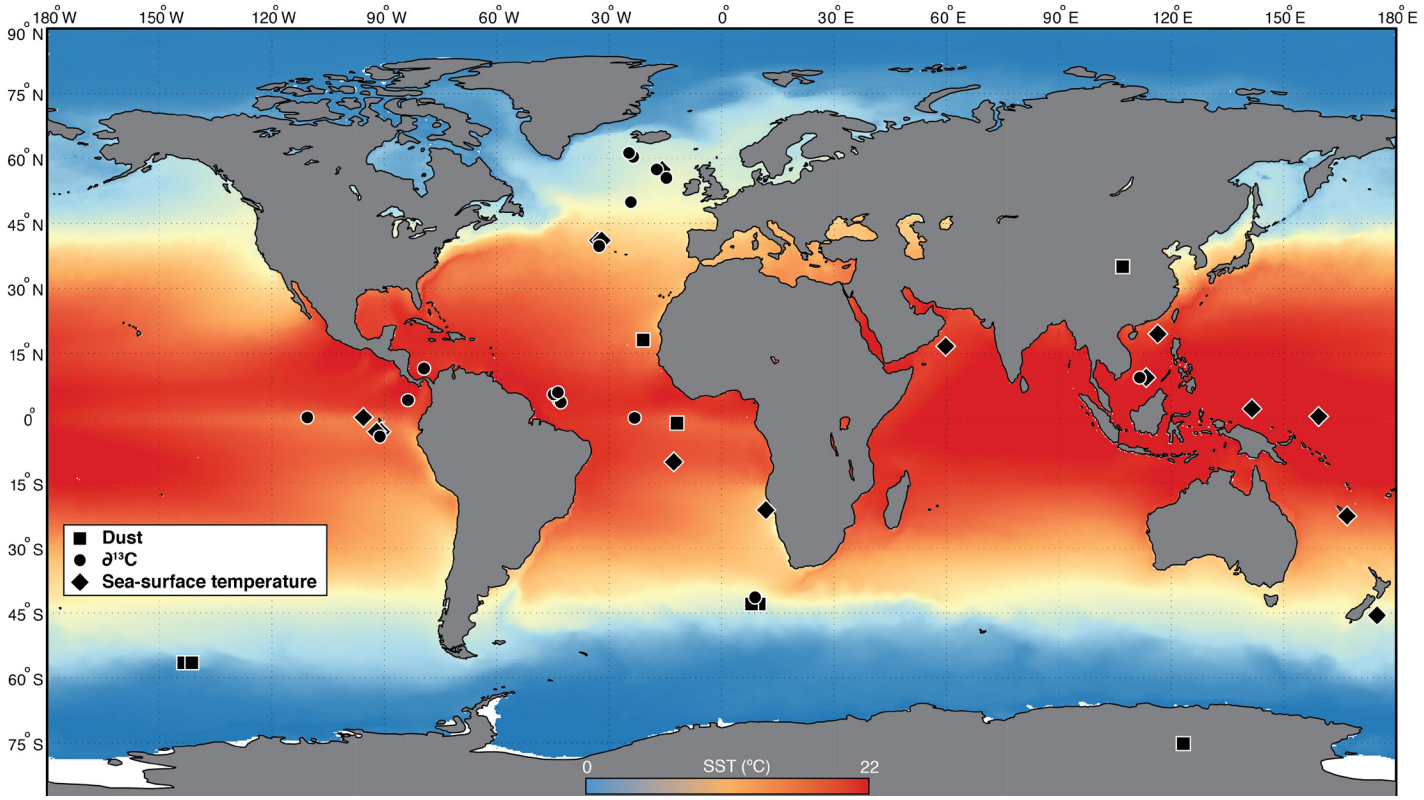

Figure 2 – Site locations. Map indicating the locations of the cores used in this research and modern sea-surface temperature values. Each symbol represents a different proxy record. Diamonds – sea-surface temperatures. Circles – benthic $\partial^{13}C$. Squares – dust.

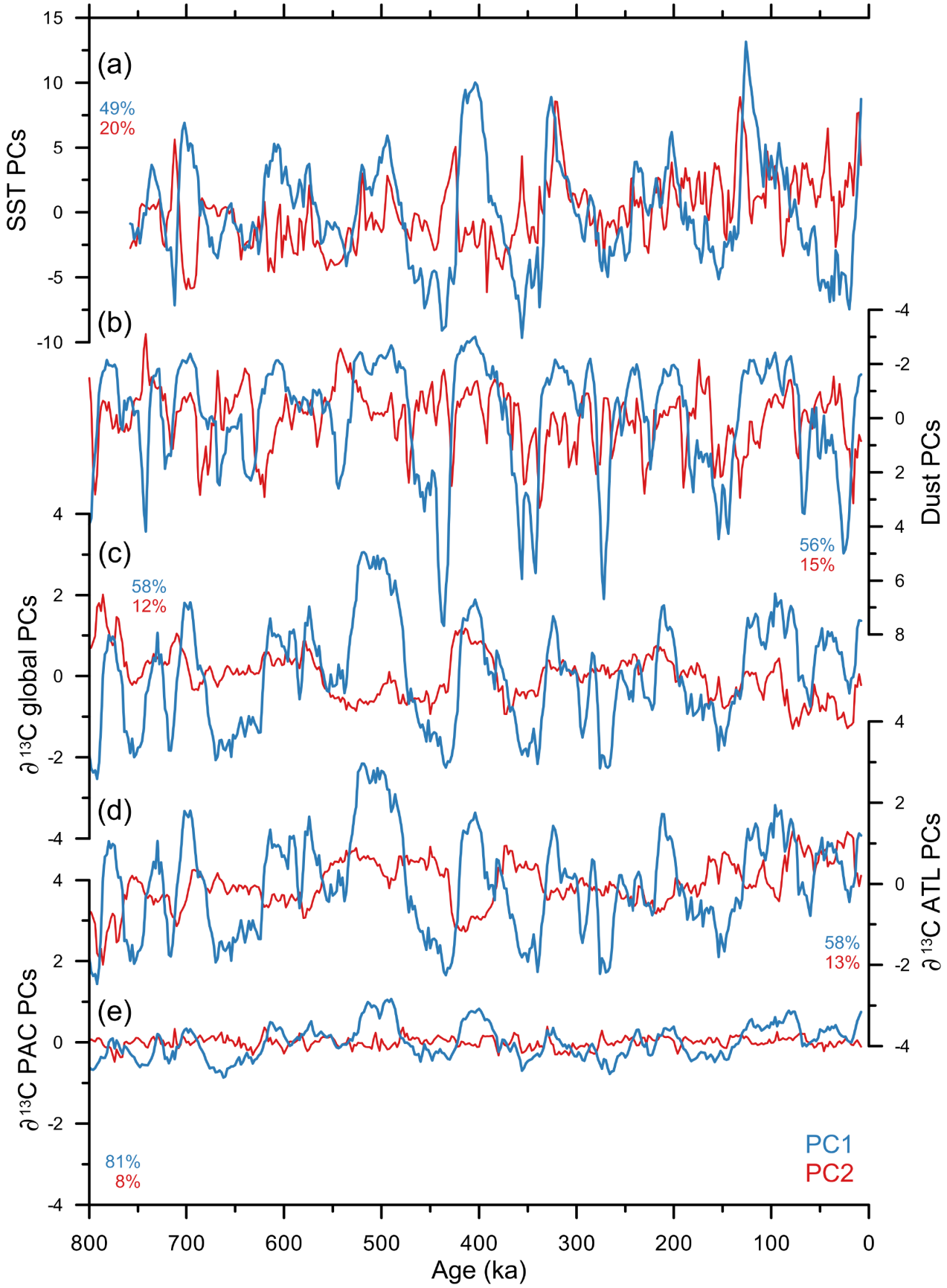

Figure 3 – Principal components. Plots of the first (PC1; blue) and second (PC2; red) principal components from our EOF analysis of each climate variable. Percent variance explained by each PC represented by the numbers with the corresponding color. **a,** Sea-surface temperatures. **b,** Dust records. **c,** Global $\partial^{13}C$. **d,** $\partial^{13}C$ of the Atlantic. **f,** $\partial^{13}C$ of the Pacific.

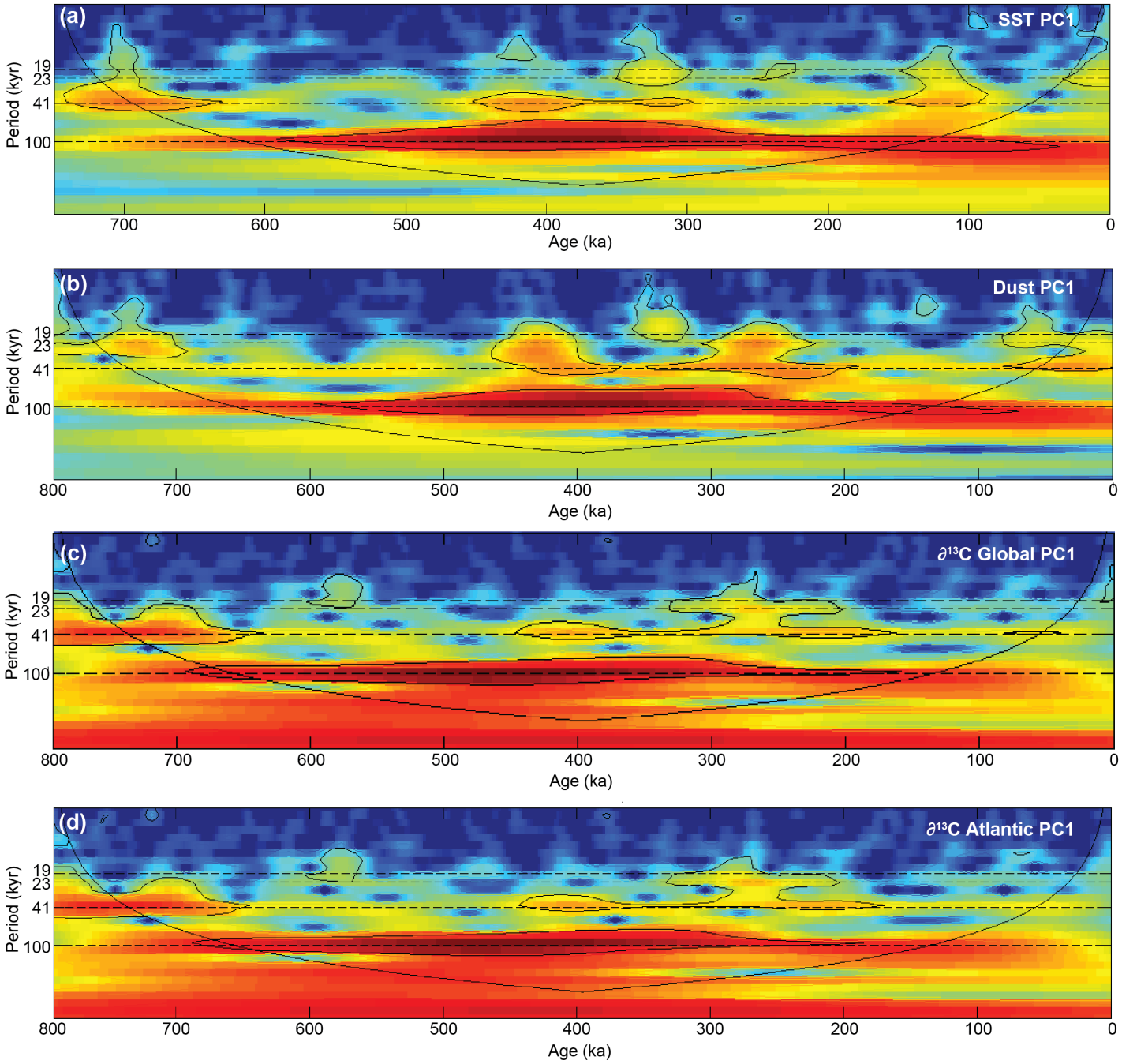

Figure 4 – Wavelet analysis. Wavelets of four of the first principal components. **a,** Sea-surface temperatures. **b,** Dust records. **c,** Global $\partial^{13}C$. **d,** $\partial^{13}C$ of the Atlantic. Red colors represent higher spectral power. Blue colors represent lower spectral power. Statistical significance highlighted by the thin black line. Milankovitch periods highlighted by the dashed horizontal lines.

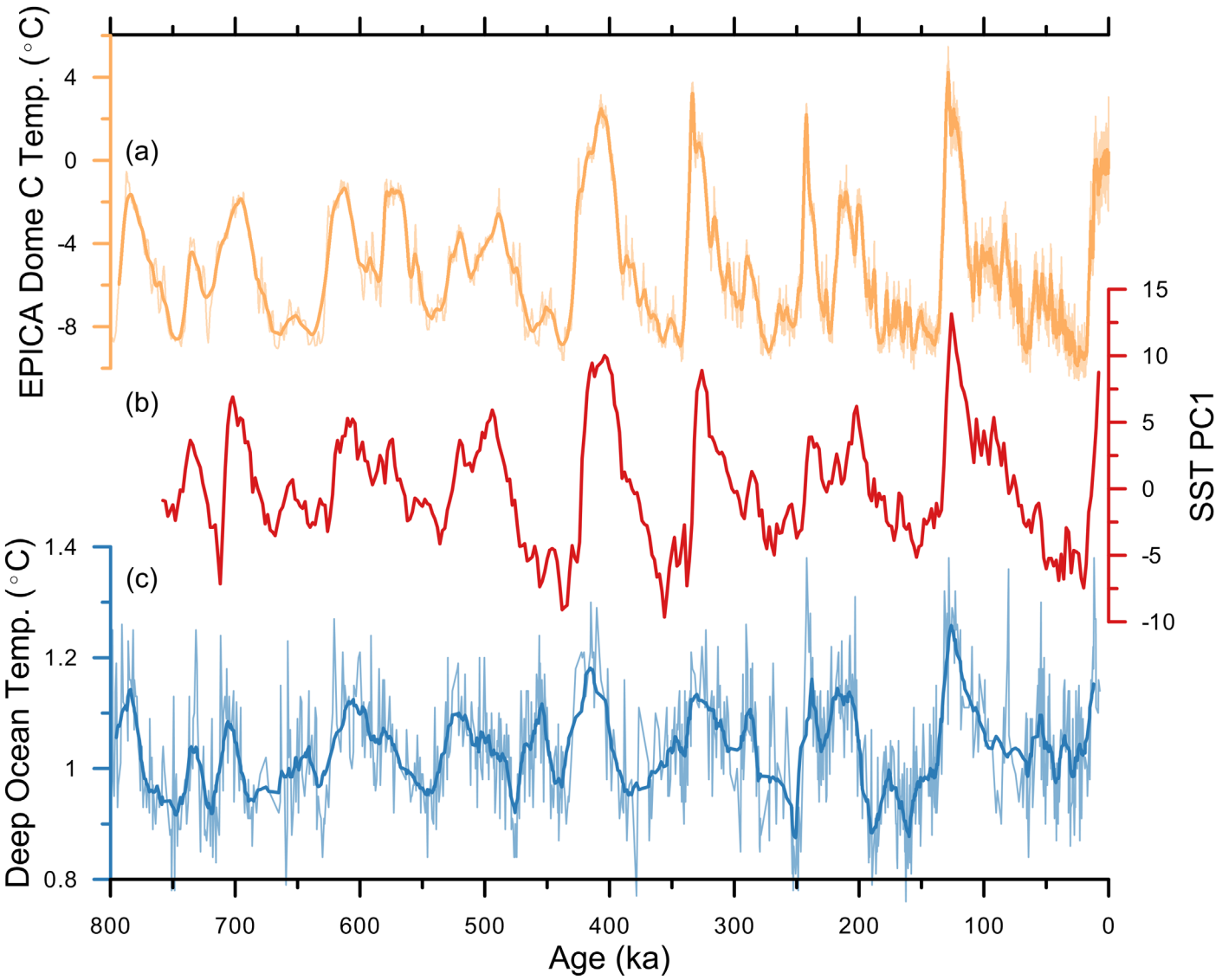

Figure 5 – Temperature records. a, Deuterium-based temperature record from EPICA Dome C in Antarctica (light yellow; Jouzel et al., 2007). The darker yellow line is a 15-point moving average. **b,** The first principal component of our sea-surface temperature analysis (red). **c,** Bottom water temperature derived from Mg/Ca measurements at ODP 1123 (light blue; Elderfield et al., 2012). Dark blue line is a 15-point moving average.

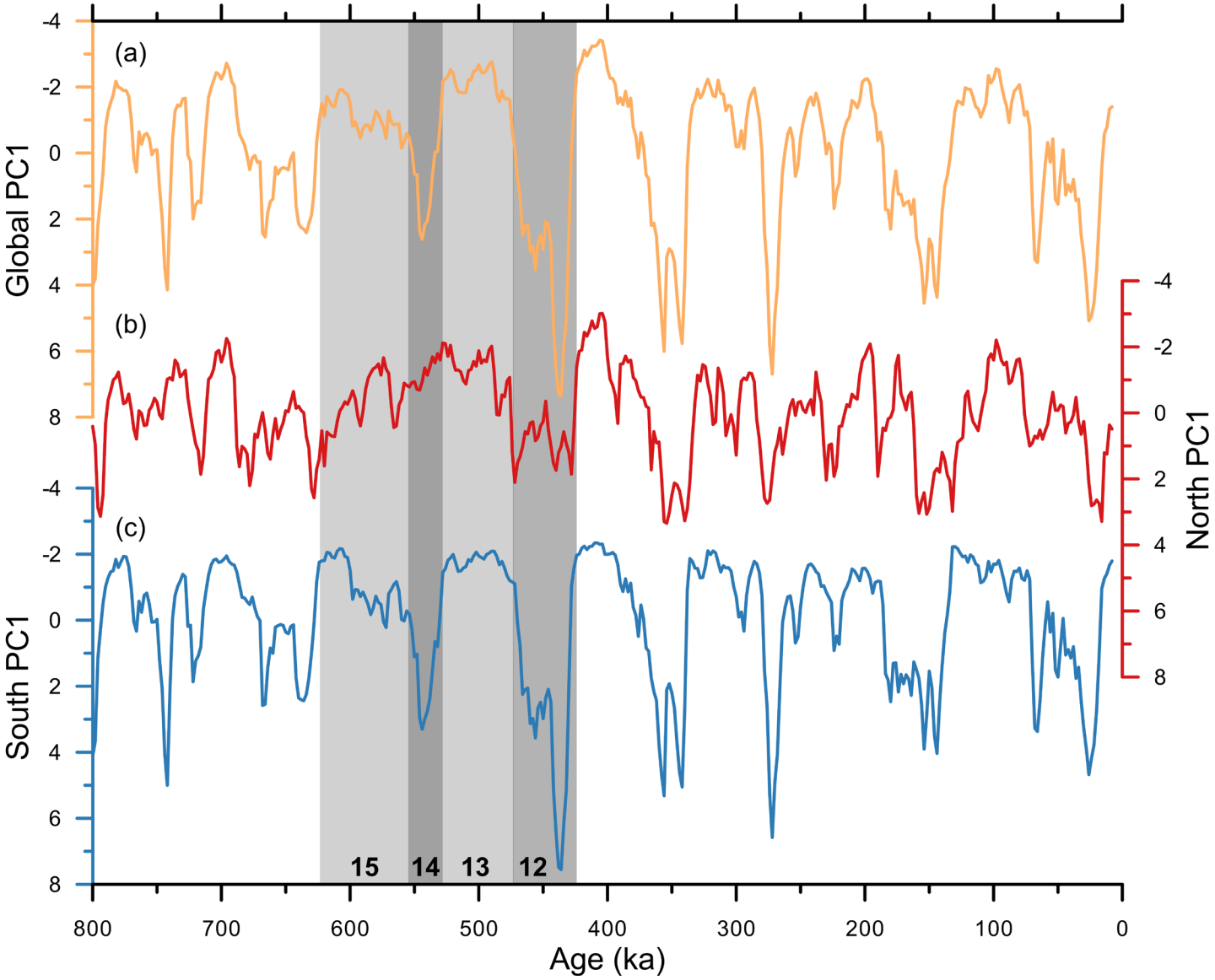

Figure 6 – Dust principal components. The first principal components of our dust analysis for the global (yellow), north (red), and south (blue) records. Vertical gray boxes highlight specific glacial (dark gray) and interglacial (light gray) periods. The numbers indicate the associated Marine Isotope Stage of each box.

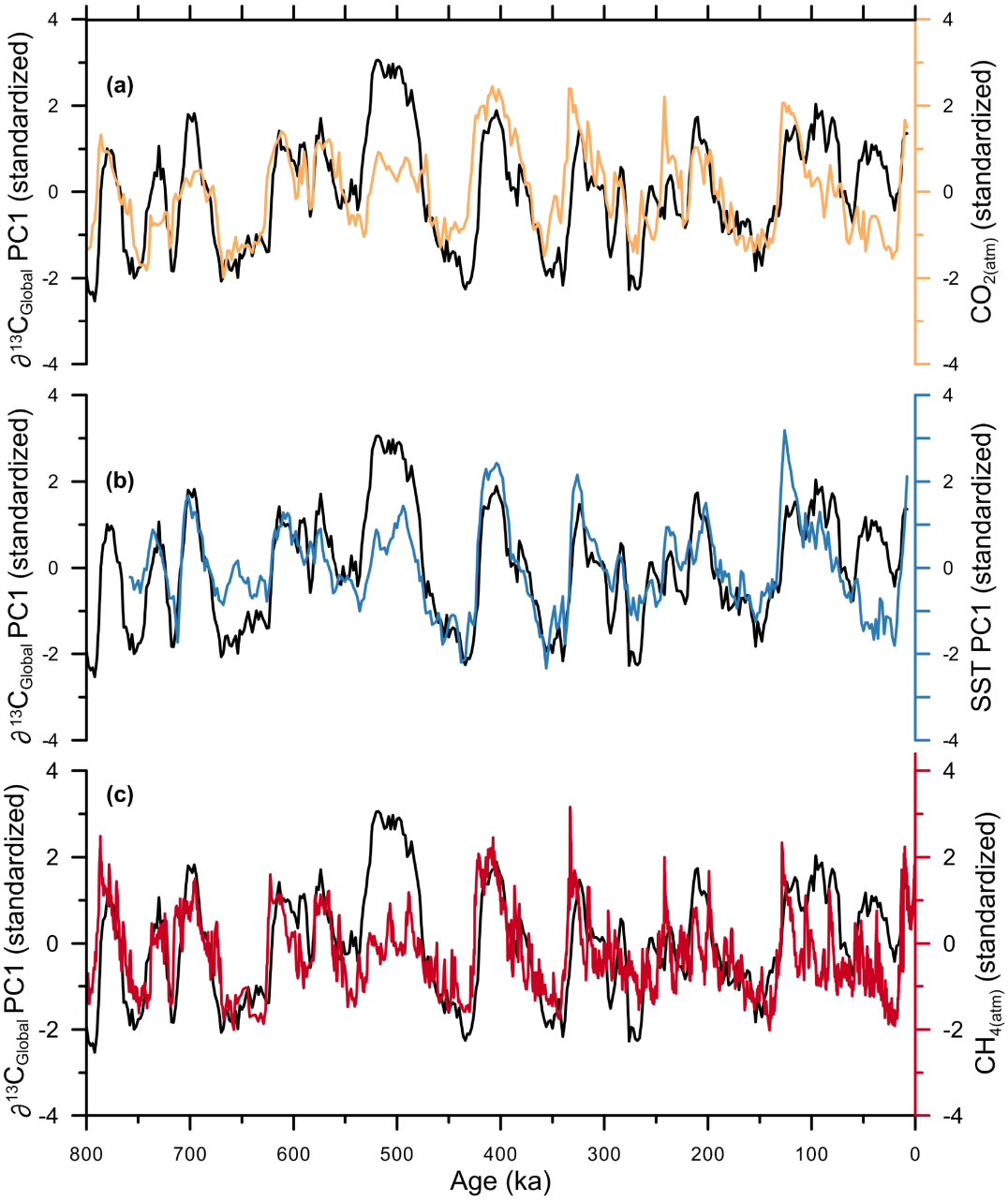

Figure 7 – Global $\partial^{13}C$ proxy comparison. Comparison of the global $\partial^{13}C$ first principal component (PC1; black) compared against **a,** EPICA Dome C CO_2 (yellow; EPICA community members, 27, Lthi et al., 28), **b,** sea-surface temperature PC1 from this research (blue), and **c,** EPICA Dome C CH_4 (red; EPICA community members, 2007).

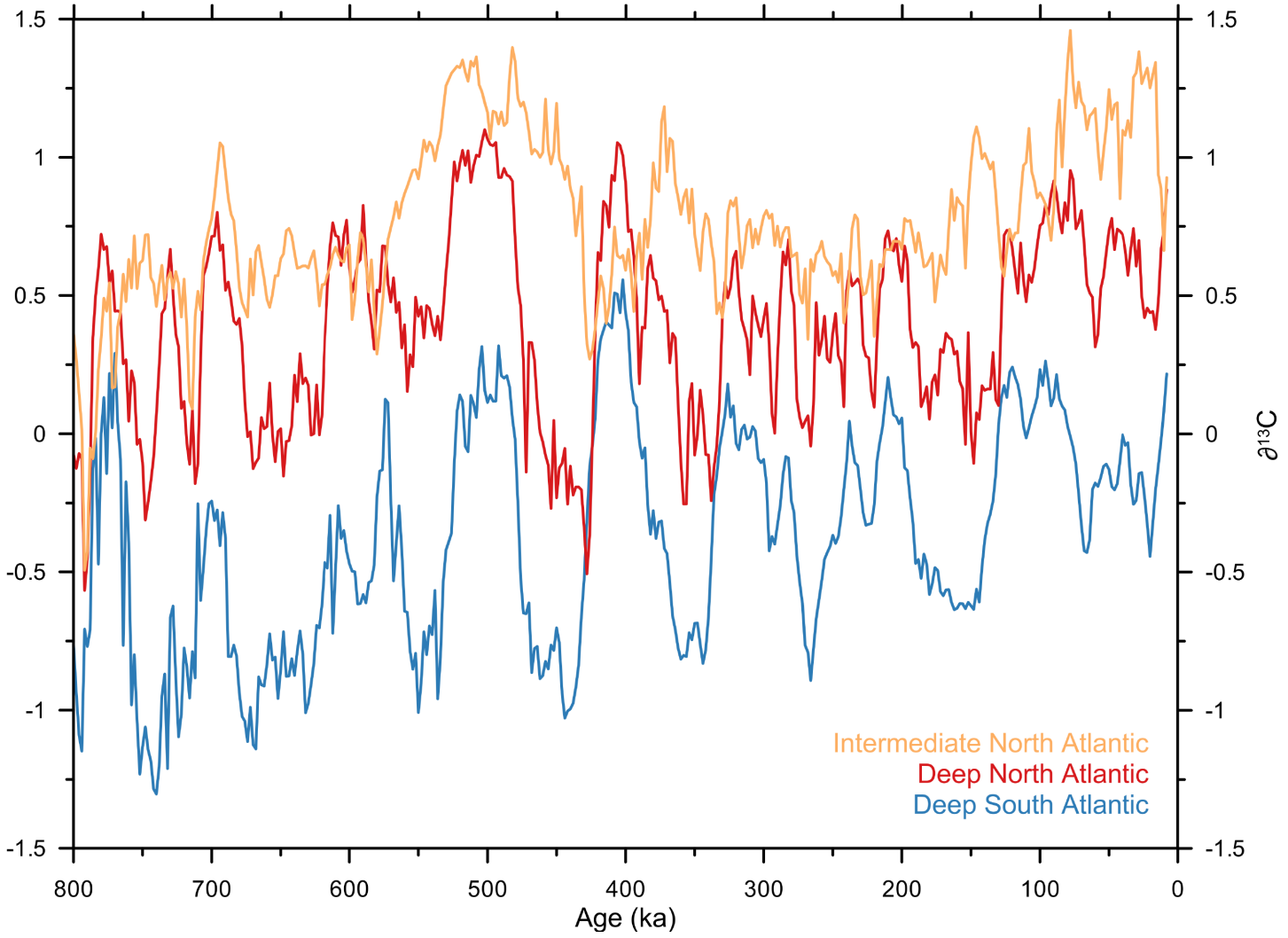

Figure 8 – Regional $\partial^{13}C$ stacks. Stacked records of benthic $\partial^{13}C$ separated into three regions: Intermediate North Atlantic (orange), Deep North Atlantic (red), and Deep South Atlantic (blue). All plots shown in $\partial^{13}C$ space to highlight different isotopic values.

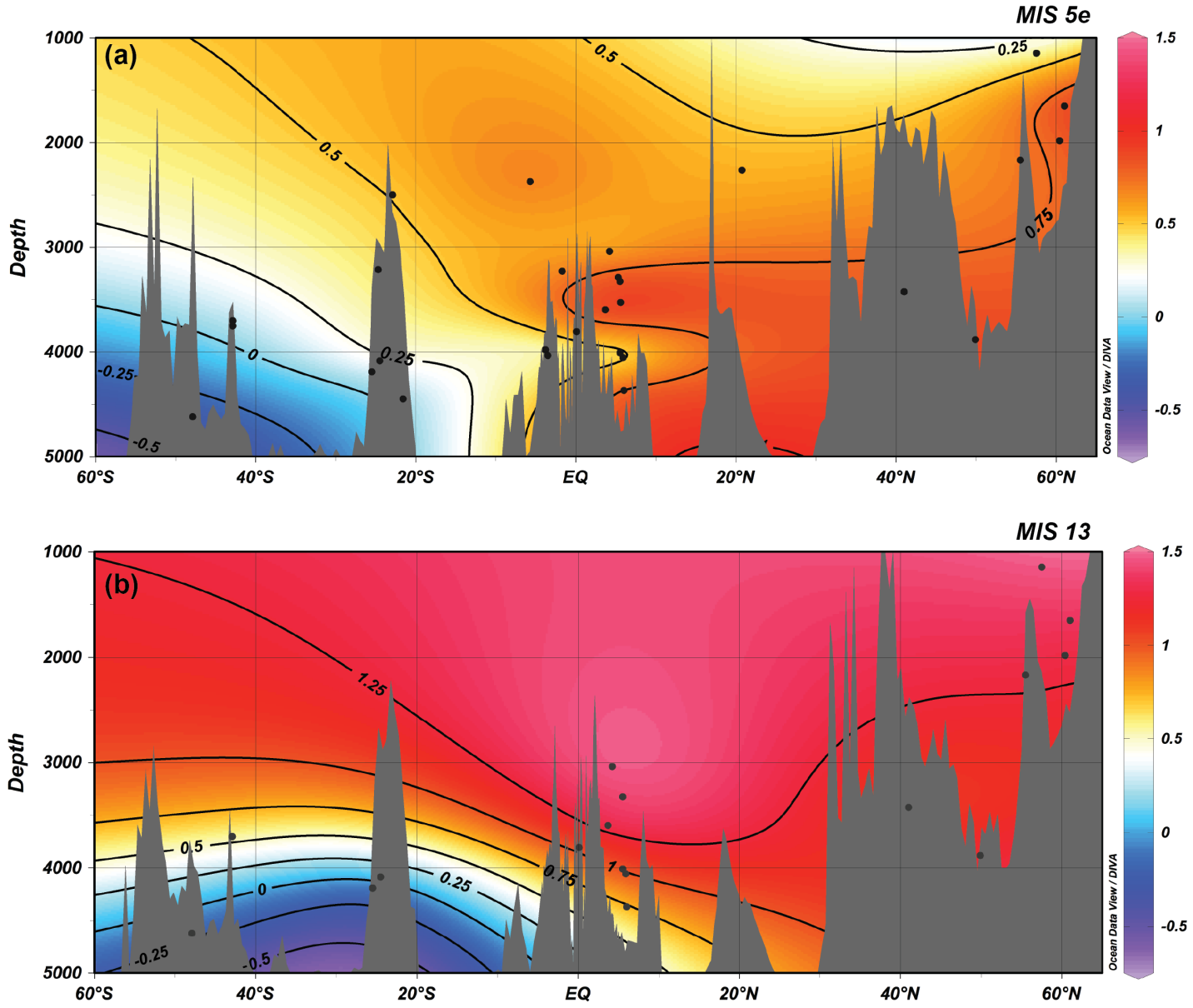

Figure 9 – MIS 13 and 5e contour plots of ∂^{13}C. Contour plots of the ∂^{13}C values in the North Atlantic basin for the interglacials MIS 13 and MIS 5e. Red colors represent more positive, enriched values. Blue colors represent lower, depleted values. Plot created using Ocean Data Viewer.

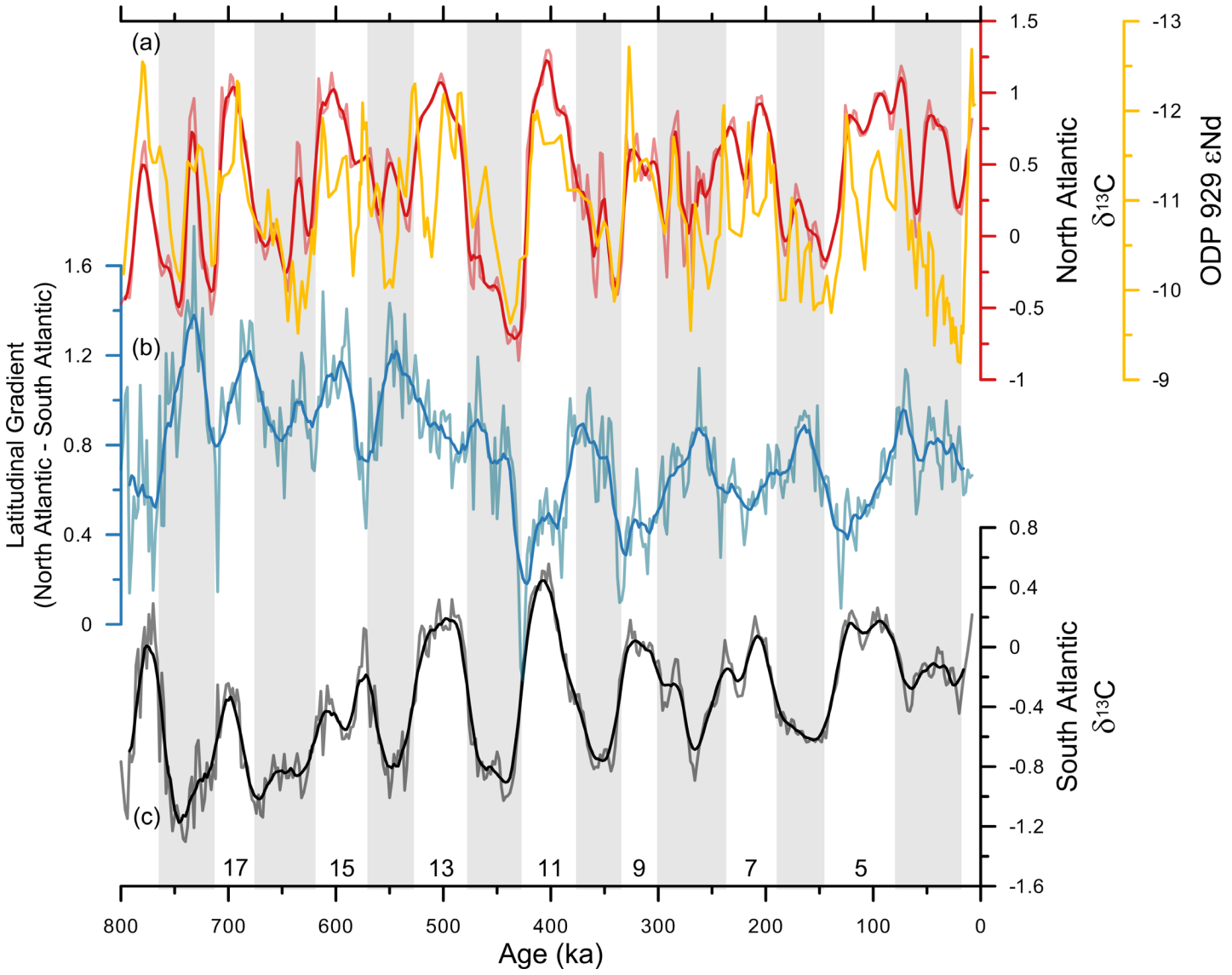

Figure 10 – Latitudinal $\partial^{13}C$ gradient. a, North Atlantic regional $\partial^{13}C$ stack plotted in $\partial^{13}C$ space (red) authigenic εNd (yellow; Howe et al., 2017). **b,** Latitudinal gradient of Atlantic $\partial^{13}C$ regional stacks (North Atlantic minus South Atlantic; blue). Lower values demonstrate increased similarity between the records. **c,** South Atlantic regional $\partial^{13}C$ stack plotted in $\partial^{13}C$ space (black). Vertical gray bars indicate glacial periods. Numbers represent Marine Isotope Stage numbers for interglacials.

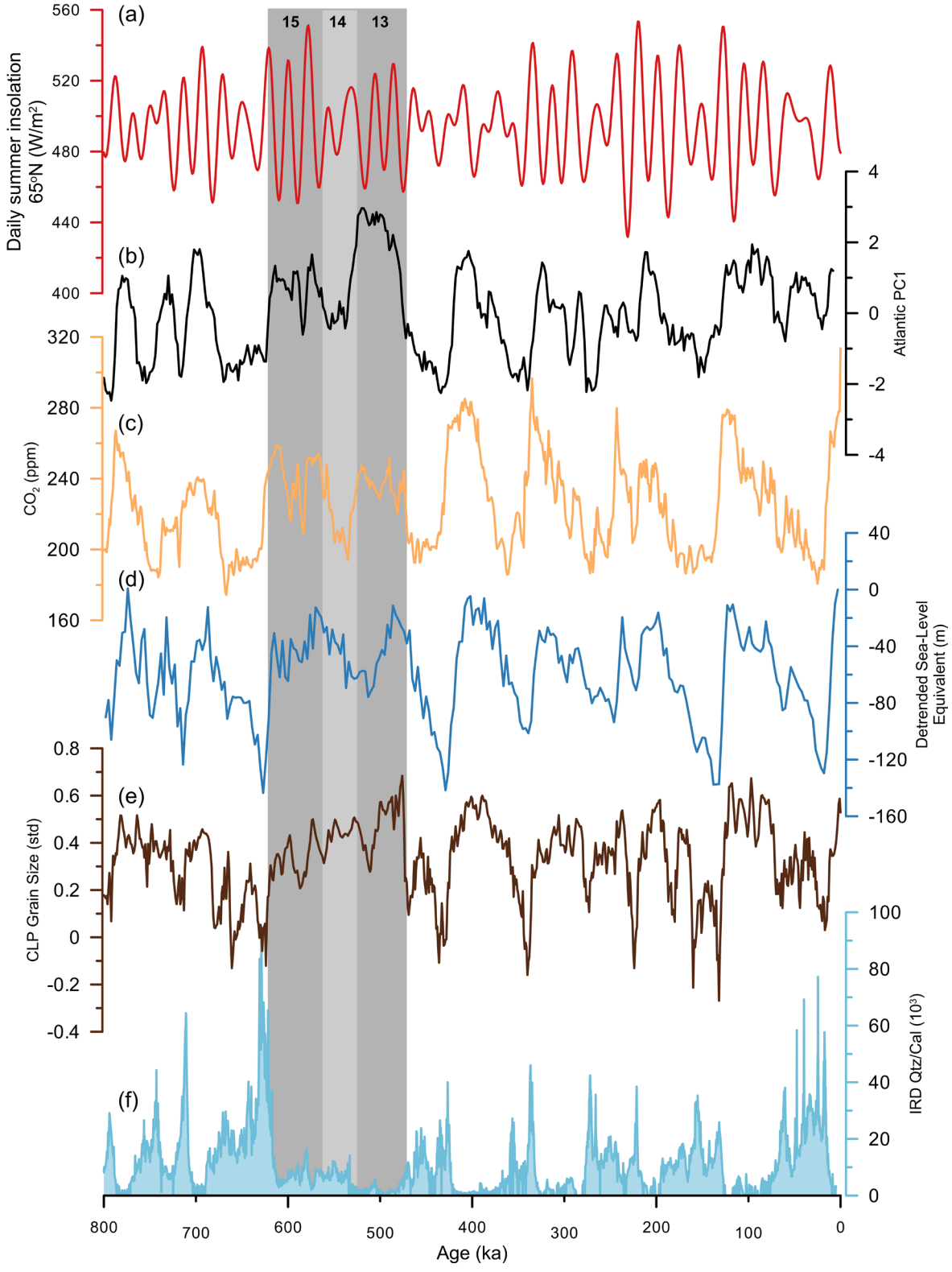

Figure 11 – Marine isotope stages 15 to 13 and the carbon isotope excursion. **a,** Summer insolation at 65º N (red). **b,** First principal component of Atlantic $\partial^{13}C$ (black). **c,** EPICA Dome C CO_2 (yellow; EPICA community members, 2004, Lüthi et al., 2008). **d,** Detrended sea-level equivalent from Shakun et al., 2015 (blue). Derived from $\partial^{18}O_{sw}$ calculations. Negative numbers indicate lower sea level and increased ice volume. **e,** Chinese Loess Plateau grain size indicating relative Asian summer monsoon strength (brown; Sun et al., 25). **f,** Quartz/Calcite ratios from site U1313 in the North Atlantic as a measure of ice-rafted debris (light blue; Naafs et al., 212). Dark gray bars highlight the interglacials (MIS 15 and MIS 13) between ~630 to ~470 ka. Light gray bar highlights MIS 14.

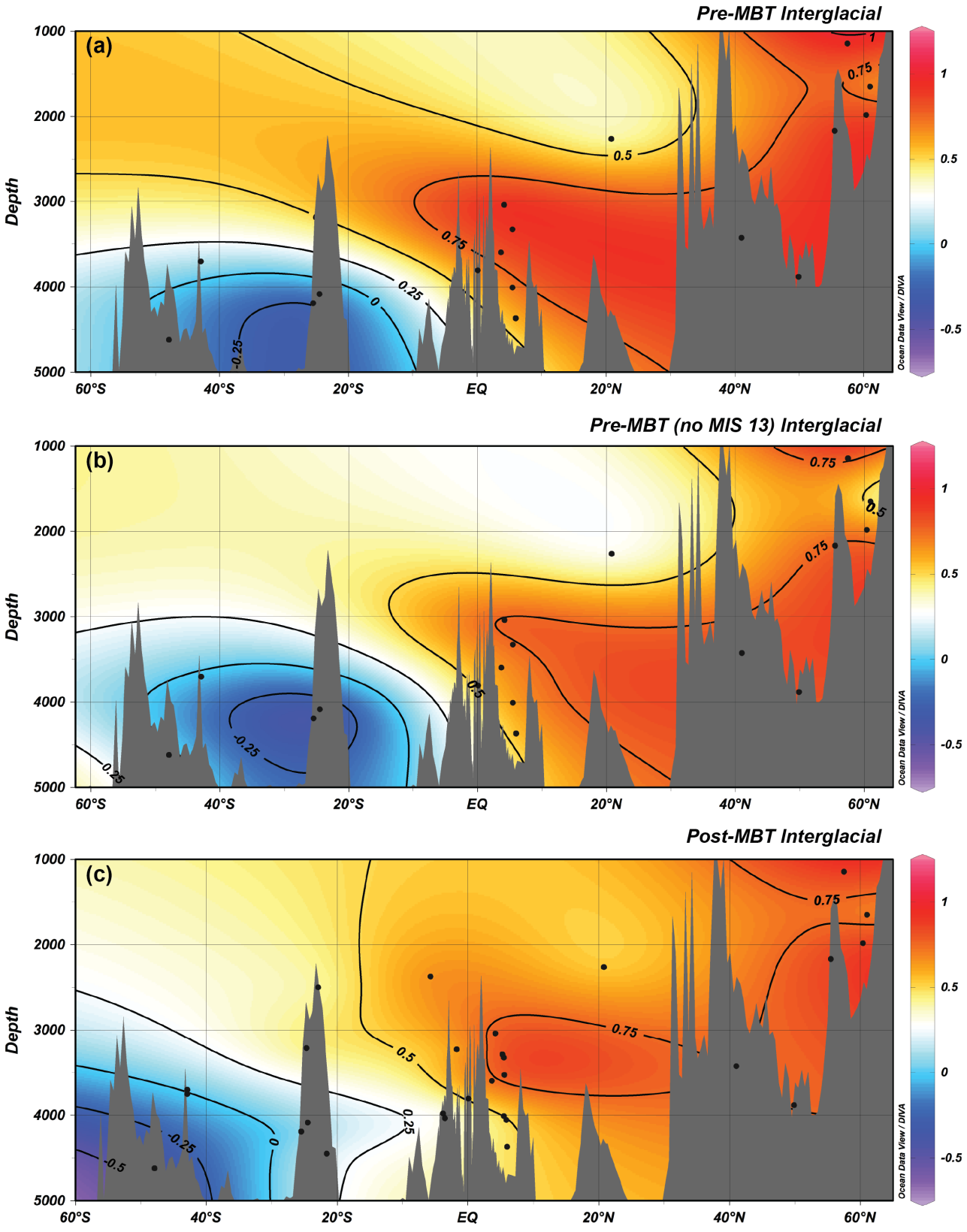

Figure 12 – Average interglacial $\partial^{13}C$ contours. Contour plots of the average interglacial $\partial^{13}C$ values in the Atlantic for **a,** pre-MBT included MIS 13, **b,** pre-MBT excluding MIS 13 (enriched carbon isotope excursion), and **c,** post-MBT. Red colors indicate higher $\partial^{13}C$ values. Blue colors indicate lower $\partial^{13}C$ values. Boundary between the two water masses (NADW and AABW) indicated at the 0.25‰ contour (Curry and Oppo, 2005).

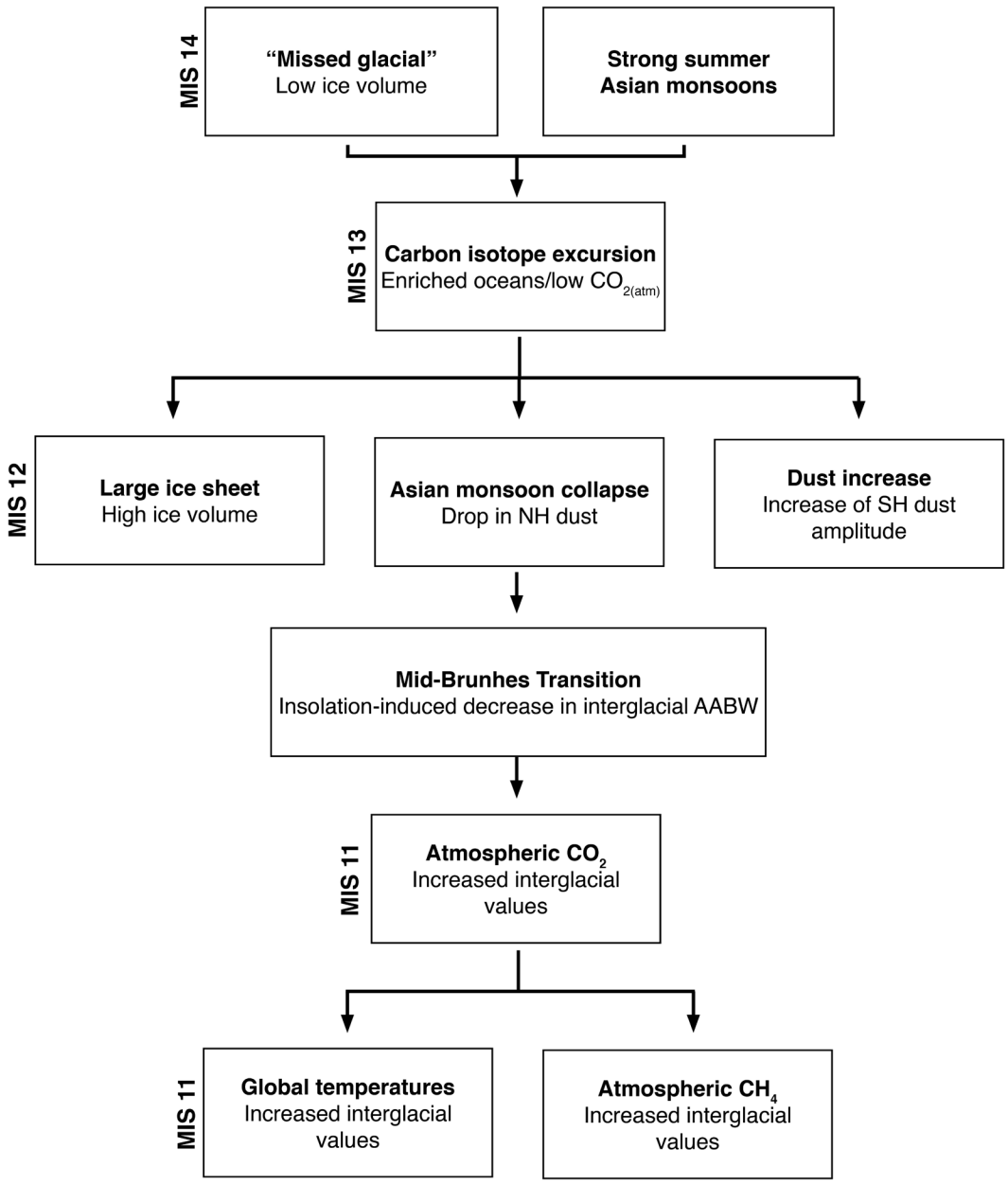

Figure 13 – Schematic representation of the sequence of events leading to the Mid-Brunhes Transition. Corresponding marine isotope stages are located on the left side of each row. Boxes in a row indicate synchronous events.

Table 1 - Data compilation

Core	Location	Latitude	Longitude	Δt (ka)	Proxy	doi/url	Reference
DSDP 607	Northeastern Atlantic	41.0012	-32.9573	2.8	SST - Transfer function	https://doi.org/10.1594/PANGAEA.701229	Ruddiman et al., 1989
ODP 846	Eastern Equatorial Pacific	-3.0949	-90.818	2.3	SST - Uk37	https://doi.org/10.1126/science.1185435	Herbert et al., 2010
ODP 982	North Atlantic	57.5165	-15.8667	4.7	SST - Uk37	https://www.ncdc.noaa.gov/paleo/study/8624	Lawrence et al., 2009
ODP 1143	Western Equatorial Pacific	9.3619	113.2851	1.9	SST - Uk37	https://doi.org/10.1594/PANGAEA.786444	Li et al., 2011
ODP 1082	South Atlantic	-21.0941	11.8205	4.5	SST - Uk37	https://doi.org/10.1594/PANGAEA.786701	Etourneau et al., 2009
ODP 1313	North Atlantic	41.0011	-32.9573	1.4	SST - Uk37	https://doi.org/10.1594/PANGAEA.744483	Naafs et al., 2012
ODP 722	Arabian Sea	16.6218	59.7953	2.0	SST - Uk37	https://doi.org/10.1126/science.1185435	Herbert et al., 2010
ODP 1146	South China Sea	19.4567	116.2727	1.6	SST - Uk37	https://doi.org/10.1126/science.1185435	Herbert et al., 2010
ODP 846	Eastern Equatorial Pacific	-3.0949	-90.818	1.3	SST - Uk37	https://doi.org/10.1038/nature02338	Liu and Herbert, 2004
MD97-2140	Western Pacific Warm Pool	2.1792	141.4581	3.9	SST - Mg/Ca	https://www.ncdc.noaa.gov/paleo/study/6266	de Garidel-Thoron, 2005
MD06-3018	Tropical Western Pacific	-22.5977	166.8628	5.2	SST - Mg/Ca	https://www.ncdc.noaa.gov/paleo/study/11188	Russon et al., 2011
ODP 806	Western Equatorial Pacific	0.319	159.361	2.4	SST - Mg/Ca	https://doi.org/10.1594/PANGAEA.772015	Medina-Elizalde and Lea, 2005
DSDP 594	Southwest Pacific	-45.5235	174.948	2.6	SST - Modern analog	https://doi.org/10.1594/PANGAEA.691478	Schaefer et al., 2005
V22-174	South Atlantic	-10.0667	-12.8167	4.1	SST - Transfer function	https://doi.org/10.1594/PANGAEA.52228	Specmap, 1990
RC13-110	Eastern Equatorial Pacific	0	-96	4.9	SST - Transfer function		Pisias et al., 1997
ODP 659	Eastern Equatorial Atlantic	18.0772	-21.0262	3.6	Dust flux	https://doi.org/10.1594/PANGAEA.696121	Tiedemann et al., 1994
ODP 1090	Subantarctic Atlantic	-42.9137	8.8997	0.3	Dust MAR	https://doi.org/10.1594/PANGAEA.767460	Martinez-Garcia et al., 2011
ODP 1090	Subantarctic Atlantic	-42.9137	8.8997	0.3	Fe MAR	https://doi.org/10.1594/PANGAEA.767460	Martinez-Garcia et al., 2011
CLP	Chinese Loess Plateau			1.0	Grain size	https://doi.org/10.1029/2006GC001287	Sun et al., 2005
Lake Baikal	Southern Russia			0.5	Silica %	https://www.ncdc.noaa.gov/paleo/study/6068	Prokopenko et al., 2006
PS75-074	Pacific Southern Ocean	-56.4696	-142.9954	0.4	Fe counts	https://doi.org/10.1594/PANGAEA.826600	Lamy et al., 2014
PS75-076	Pacific Southern Ocean	-56.4696	-142.9954	0.4	Fe wt. %	https://doi.org/10.1594/PANGAEA.826600	Lamy et al., 2014
ODP 663	Eastern Equatorial Atlantic	-1.1978	-11.8785	2.7	Terrestrial %	https://doi.org/10.1594/PANGAEA.208129	deMenocal et al., 1993
EPICA Dome C	Antarctica	-75.06	123.21	0.2	Dust	https://doi.org/10.1594/PANGAEA.695995	Lambert et al., 2008
ODP 982	North Atlantic	57.5	-15.9	2.5	$\partial^{13}C$	https://doi.org/10.1594/PANGAEA.700897	Venz et al., 1999
ODP 983	North Atlantic	60.4	-23.6	1.0	$\partial^{13}C$	https://www.ncdc.noaa.gov/paleo/study/2543	McIntyre et al., 1999
ODP 984	North Atlantic	61	-24	3.5	$\partial^{13}C$	https://www.ncdc.noaa.gov/paleo/study/5897	Raymo et al., 2004
DSDP 607	North Atlantic	41	-33	4.1	$\partial^{13}C$	https://doi.org/10.1594/PANGAEA.52379	Ruddiman et al., 1989
ODP 658	North Atlantic	20.8	-18.7	1.6	$\partial^{13}C$	https://doi.org/10.1594/PANGAEA.68570	Tiedmann et al., 1994
U 1308	North Atlantic	49.9	-24.2	0.3	$\partial^{13}C$	https://www.ncdc.noaa.gov/paleo/study/10250	Hodell et al., 2008
ODP 980/981	North Atlantic	55.5	-14.7	1.6	$\partial^{13}C$	https://doi.org/10.1594/PANGAEA.698998	Oppo et al., 1998
DSDP 502	Equatorial Atlantic	11.5	-79.4		$\partial^{13}C$	https://doi.org/10.1594/PANGAEA.701470	deMenocal et al. 1992
ODP 664	Equatorial Atlantic	0.1	-23.2	3.2	$\partial^{13}C$	https://www.ncdc.noaa.gov/paleo/study/2529	Raymo et al., 1997
ODP 925	Equatorial Atlantic	4.2	-43.5	4.3	$\partial^{13}C$		Bickert et al., 1997
ODP 926	Equatorial Atlantic	3.7	-42.9	2.7	$\partial^{13}C$		Lisiecki et al., 2008
ODP 927	Equatorial Atlantic	5.5	-44.5		$\partial^{13}C$		Bickert et al., 1997
ODP 929	Equatorial Atlantic	5.5	-44.5	4.9	$\partial^{13}C$		Bickert et al., 1997
ODP 928	Equatorial Atlantic	5.5	-44.8	2.5	$\partial^{13}C$		Lisiecki et al., 2008
ODP 1090	South Atlantic	-42.9	8.9	2.8	$\partial^{13}C$	https://doi.org/10.1594/PANGAEA.696106	Venz and Hodell, 2002
GeoB 1032	South Atlantic	-22.9	6	3.7	$\partial^{13}C$	https://doi.org/10.1594/PANGAEA.54655	Wefer et al., 1996
GeoB 1035	South Atlantic	-21.6	5	3.9	$\partial^{13}C$	https://doi.org/10.1594/PANGAEA.58766	Bickert and Wefer, 1996
ODP 1089	South Atlantic	-47.9	9.9	0.4	$\partial^{13}C$	https://doi.org/10.1594/PANGAEA.701432	Hodell et al., 2003
GeoB 1211	South Atlantic	-24.5	7.5	4.9	$\partial^{13}C$	https://doi.org/10.1594/PANGAEA.103634	Bickert and Wefer, 1996
GeoB 1214	South Atlantic	-24.7	7.2	4.5	$\partial^{13}C$	https://doi.org/10.1594/PANGAEA.103635	Bickert and Wefer, 1996
RC13-229	South Atlantic	-25.5	11.3	3.8	$\partial^{13}C$	https://doi.org/10.1594/PANGAEA.701361	Oppo et al., 1990
TN 576	South Atlantic	-42.9	8.9	1.5	$\partial^{13}C$	https://www.ncdc.noaa.gov/paleo/study/2576	Hodell et al., 2000
ODP 1143	Pacific	9.4	-246.7	3.8	$\partial^{13}C$	https://doi.org/10.1594/PANGAEA.784150	Cheng et al., 2004
ODP 677	Pacific	4.2	-83.7	2.8	$\partial^{13}C$	https://doi.org/10.1594/PANGAEA.701316	Shackleton et al., 1990
ODP 846	Pacific	-3.1	-90.8	2.2	$\partial^{13}C$	https://doi.org/10.1594/PANGAEA.808207	Mix et al., 1995
ODP 849	Pacific	0.2	-110.5	3.5	$\partial^{13}C$	https://doi.org/10.1594/PANGAEA.701400	Mix et al., 1995
ODP 1123	Southwest Pacific	-41.7862	-171.499	0.8	Mg/Ca	https://doi.org/10.1594/PANGAEA.786205	Elderfield et al., 2012
EPICA Dome C	Antarctica	-75.06	123.21	0.4	CH_4	https://www.ncdc.noaa.gov/paleo/study/6093	Loulergue et al., 2008
EPICA Dome C	Antarctica	-75.06	123.21	0.4	CO_2	https://www.ncdc.noaa.gov/paleo/study/6091	Luthi et al., 2008
EPICA Dome C	Antarctica	-75.06	123.21	3.0	Deuterium	https://www.ncdc.noaa.gov/paleo/study/6080	EPICA Community Members, 2004